

# Equation of State Calculations of Hydrogen-Helium Mixtures in Solar and Extrasolar Giant Planets

Burkhard Militzer<sup>1</sup>

<sup>1</sup>*Department of Earth and Planetary Science, Department of Astronomy, University of California, Berkeley*

Using density functional molecular dynamics simulations, we study the equation of state for hydrogen-helium mixtures at conditions of giant planet interiors of  $0.2\text{--}2.3\text{ g cm}^{-3}$  and  $1000\text{--}80000\text{ K}$  for a typical helium mass fraction of 0.245. In addition to computing internal energy and pressure, we determine the entropy by applying a thermodynamic integration technique in the presence of electronic excitations. We extend this technique to include the dissociations and recombination of hydrogen molecules. Results are compared to the widely used analytic model by Saumon and Chabrier. We also report evidence of spontaneous hydrogen-helium phase separation in simulations at low temperature and high density.

PACS numbers:

## I. INTRODUCTION

The Kepler mission has provided us with over 2000 exoplanet candidates<sup>1</sup> that vary widely in composition and span a wide range of orbital parameters. In 2016, the Juno mission is expected to provide us with high precision gravity and magnetic field measurements for Jupiter that will yield strong constraints on the interior structure of this planet. Despite great progress, high pressure experiments<sup>2</sup> cannot yet reach high enough densities to characterize a large part of the interiors of giant planets<sup>3</sup>. In this paper, we will make a contribution to the understanding of giant planet interiors by computing the equation of state (EOS) of hydrogen-helium mixtures (HHM) from density functional molecular dynamics (DFT-MD) simulations.

While determining pressure and internal energy from DFT-MD simulations is straightforward, the entropy is not directly accessible. Because giant planets cool convectively, their interior temperature profile follows an adiabat. An accurate knowledge of the entropy of HHM at high pressure is therefore of crucial importance for determining the temperature profile, the density, and the budget of thermal energy stored in the interior of a planet. In 2008, two groups constructed Jupiter interior models from DFT-MD simulations<sup>4,5</sup>. While the derived pressures and internal energies can be considered to be more reliable than analytical EOS models by Saumon and Chabrier (SC)<sup>6</sup>, both papers predicted very different interior temperature profiles for Jupiter<sup>7</sup>. As we will show here, the work by Nettelmann *et al.*<sup>5</sup> overestimated the temperature at Jupiter's core-mantle boundary (CMB) by 3050 K while we underestimated it by 2870 K<sup>4</sup>. The corrections to the SC EOS model are in fact only  $-350\text{ K}$ .

## II. COMPUTATIONAL METHODS

In Refs. [4,5], the entropy has been inferred by computing free energy differences such as  $F(V_2) - F(V_1) = \int P dV$  or,  $F(T_2) - \beta_1 F(T_1) = \int d\beta E(\beta)$  with  $\beta = 1/k_b T$ . With DFT-MD one can, however, only derive  $P$  and  $E$  with a statistical uncertainty for a finite number of  $(T, \rho)$  grid points. Recently, Nettelmann *et al.*<sup>8</sup> added more  $P$  and  $E$  points to an existing table. Nevertheless, it is difficult to find a starting point

for the integration where the free energy is known analytically. In the molecular low-density limit, the required simulation volumes are so large that plane wave based DFT-MD simulations become very inefficient. At very high density, where analytical model for degenerate plasmas work well, pseudopotentials<sup>9</sup> may no longer work without special care. One is consequently better off deriving the free energy with a method that does not require the integration over a large  $(T, \rho)$  range where HHM may undergo substantial thermodynamic changes. Alternatively, the Helmholtz free energy of dense many-body systems can be derived with a thermodynamic integration (TDI) technique where one switches between DFT and classical forces<sup>10-14</sup>,

$$F_{\text{DFT}} - F_{\text{cl}} = \int_0^1 d\lambda \langle V_{\text{KS}} - V_{\text{cl}} \rangle_\lambda. \quad (1)$$

The angle brackets represent an average over trajectories governed by forces that are derived from a hybrid potential energy function,  $V_\lambda = \lambda V_{\text{KS}} + (1 - \lambda)V_{\text{cl}}$ .  $V_{\text{cl}}$  is the potential energy of the classical system and  $V_{\text{KS}}$  is the Kohn-Sham energy. The sum of  $V_\lambda$  and the kinetic energy of the ions,  $K_{\text{ion}}$ , is constant in microcanonical simulations. For each density and temperature under consideration, we construct a classical reference system by fitting a pair potentials between each pair of atomic species to the DFT-MD forces using a force matching approach and spline functions<sup>15</sup>. The free energy of the classical reference system,  $F_{\text{cl}}$ , is obtained with Monte Carlo simulations and TDI to a system of non-interacting particles.

This TDI technique provides us with an efficient and accurate way to determine the ionic contributions to the entropy,  $TS_{\text{ion}} = \langle V_{\text{KS}} \rangle + \langle K_{\text{ion}} \rangle - F_{\text{DFT}}$ , which is an excellent measure of the entropy of the whole system in most cases. However, in the hot interiors of exoplanets, electronic excitations become important. They can be accounted for following the work by Wijs *et al.*<sup>16</sup>. First, the finite temperature Fermi occupation of electronic states according to the Mermin functional<sup>17</sup> affects the MD trajectories<sup>18</sup> because the forces are derived from an instantaneous Mermin free energy<sup>19</sup>,  $\Omega = V_{\text{KS}} - TS_{\text{el}}$ . This implies that  $\Omega$  replaces  $V_{\text{KS}}$  in all preceding equations.  $\Omega + K_{\text{ion}}$  becomes the new constant of motion in microcanonical simulations. Subsequently, the term,  $TS_{\text{el}} = V_{\text{KS}} - \Omega$ , represents the intrinsic contributions from the electrons to the entropy of the system. By

adding the ionic and electronic terms, one obtains the following expression for the total entropy of a system with electronic excitations,

$$T(S_{\text{ion}} + S_{\text{el}}) = \langle V_{\text{KS}} \rangle + \langle K_{\text{ion}} \rangle - \int_0^1 d\lambda \langle \Omega - V_{\text{cl}} \rangle_\lambda - F_{\text{cl}}. \quad (2)$$

$\langle V_{\text{KS}} \rangle$  includes contributions from partially occupied excited states. We tested this method by computing the Gibbs free energies at  $T_1 = 10\,000$  K and  $T_2 = 80\,000$  K where substantial electronic excitations are present. We found agreement within the error bars when we compared the results with the values obtained from  $\beta_2 F(T_2) - \beta_1 F(T_1) = \int d\beta E(\beta)$ .

For molecular hydrogen, we need to construct a different classical reference system because matched pair forces alone lead to the formation of unphysical clusters of atoms. We thus introduced a force model that distinguishes between an intramolecular and an intermolecular pair potential between hydrogen atoms,  $V_{\text{mol}}$  and  $V_{\text{inter}}$ . After pairing up the closest hydrogen atoms for series of configurations, we fitted both potentials with a force-matching method.

Since hydrogen exchange reactions occur in dense molecular hydrogen already at 3000 K, we also accounted for dissociation and recombination events in our force model by dynamically determining whether two hydrogen atoms primarily interact via the  $V_{\text{mol}}$  or the  $V_{\text{inter}}$  potential. The total potential energy of our revised force model reads,

$$V = \sum_{i,j,i>j} g_{ij} V_{\text{mol}}(r_{ij}) + (1 - g_{ij}) V_{\text{inter}}(r_{ij}), \quad (3)$$

$$g_{ij} = p_{ij} f(s_i + s_j, s^*, \beta), \quad s_i = \sum_{j,j \neq i} p_{ij}, \quad (4)$$

$$p_{ij} = f(r_{ij}, r^*, \alpha), \quad r_{ij} = r_i - r_j \quad (5)$$

The function,  $f(x, x^*, \eta) = \{1 - \tanh[\eta(x - x^*)]\}/2$ , smoothly switches between 0 and 1 and serves two purposes. First, setting the parameters,  $r^* = 1.2 \text{ \AA}$  and  $\alpha = 4 \text{ \AA}^{-1}$ , determines the distance range for a bond to be considered molecular. Secondly, specifying  $s^* = 2$  and  $\beta = 1$  prevents the formation of unphysical hydrogen clusters in particular  $\text{H}_3$ . If the coordination number of an atom,  $s_i$ , exceeds 1, the molecular character of all of its bonds is reduced, which introduces a significant energy penalty that represents Pauli exclusion effects during collisions between molecules.

This construction allows for dissociation and hydrogen exchange reactions to occur while the over-coordination penalty guarantees that no hydrogen atom is bonded to more than one other atom at a time. With this force field, we obtained a stable and accurate thermodynamic integration procedure for pure molecular hydrogen and mixtures with helium. This method also works well at high temperature where no molecules are stable but some short-lived bonds exist. The DFT free energies that we obtained for  $r_s = 1.86$  and 10 000 K with the TDI method using this dynamic dissociation model agreed within error bars with our TDI results based on the original classical reference system with the pair forces only.

As a final step, we need to discuss how we add the quantum effects in the motion of nuclei to our DFT-MD results that

$N_H$	$k$ points	$S(k_b/\text{el.})$	$\Delta T(K)$
128	$\Gamma$	7.550(17)	393(9)
128	$(\frac{1}{4}, \frac{1}{4}, \frac{1}{4})$	7.508(20)	170(10)
128	$2 \times 2 \times 2$	7.512(24)	194(13)
256	$(\frac{1}{4}, \frac{1}{4}, \frac{1}{4})$	7.494(17)	98(9)
256†	$(\frac{1}{4}, \frac{1}{4}, \frac{1}{4})$	7.492(20)	88(11)
256‡	$(\frac{1}{4}, \frac{1}{4}, \frac{1}{4})$	7.483(20)	42(11)
256	$2 \times 2 \times 2$	7.493(28)	92(15)
512	$(\frac{1}{4}, \frac{1}{4}, \frac{1}{4})$	7.498(21)	120(11)

TABLE I: Pressure and entropy of pure hydrogen at 10 000 K and  $r_s=1.1$  derived from simulations with different numbers of particles,  $N_H$ , and k-point grids. All simulations used GGA except for ‡ that used LDA. No electronic excitations were included except for †.

treat all nuclei classically. After evaluating a number of different approaches, we decided to derive the quantum correction due to molecular vibrations from the intramolecular pair potentials,  $V_{\text{mol}}$ , that we have already derived. We derive the difference between the quantum and the classical entropy by solving a 1D problem through exact diagonalization. Since the  $V_{\text{mol}}$  potentials are derived from the DFT-MD forces for a given density and temperature, our approach captures some of the interaction effects among hydrogen molecules and with helium atoms. It becomes exact in the low density limit.

All simulations were performed with the VASP code<sup>20</sup> with pseudopotentials of the projector-augmented wave type<sup>9</sup>, a cutoff for the expansion of the plane wave basis set for the wavefunctions of at least 1000 eV, and the PBE exchange-correlation functional<sup>21</sup>.

### III. RESULTS AND DISCUSSION

We begin the discussion of our results with an analysis of finite size errors in simulations of pure hydrogen at  $r_s=1.1$  and 10 000 K in order to determine the temperature deep in Jupiter's interior with high accuracy. Table I compares the entropy derived from simulations with 128, 256, and 512 hydrogen atoms and various k-points sets. The deviation from the SC prediction of  $S_{\text{SC}} = 7.475 k_b/\text{el.}$  is then converted to a temperature correction of the SC adiabat using  $\Delta T = \frac{\partial T}{\partial S}|_V (S_{\text{DFT}} - S_{\text{SC}})$ . The correction is surprisingly small compared to <sup>4,5</sup>. One finds that 128 atoms are insufficiently small while results from simulations with 256 and 512 atoms agree within our  $1\sigma$  error bars. The effects of a  $2 \times 2 \times 2$  sampling of the Brillouin zone can already be captured by using Baldereschi<sup>5</sup> zone-average point,  $k = (\frac{1}{4}, \frac{1}{4}, \frac{1}{4})$ . The differences between the local density approximation (LDA) and PBE are too small to matter for giant planet interior models. Electronic excitations do not matter for Jupiter's interior, confirming<sup>4</sup>, but are important for hotter exoplanets.

Figure 1 compares the computed entropies up to 5000 K as a function of the Wigner-Seitz radius,  $r_s$ , defined as  $\frac{4}{3}\pi r_s^3 = V/N_e$  and reported in Bohr radii. For 5000 K, we find good agreement with the SC model at the highest density where

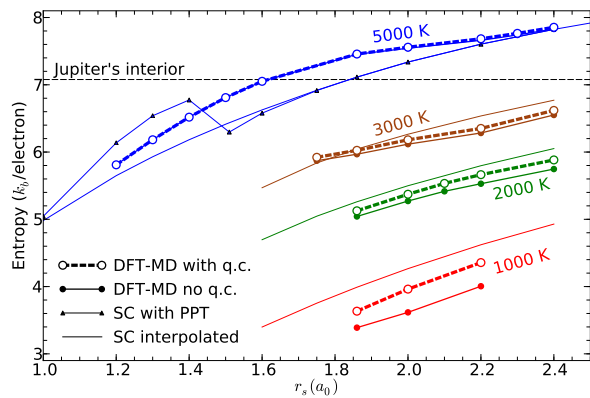


FIG. 1: Entropy of HHM derived from DFT-MD with and without nuclear quantum corrections are compared with the SC model with the plasma phase transition (PPT) and the interpolated version.

the system is dense and degenerate and also at the low density where still carries a molecular signature but the hydrogen molecules frequently dissociate and recombine due to the high temperature. At intermediate densities we find deviations up to  $0.4 k_b$  per electron at 5000 K between SC and DFT-MD.

Simulations at lower temperature between 1000 and 3000 K, where the hydrogen molecules have significantly longer lifetimes, show very similar behavior for the entropy as function of density but the DFT-MD and SC curves appear to be offset. Quantum corrections are important in the molecular regime. They reduce the deviation between DFT-MD simulations and the SC model but small deviations remain. Interactions between molecules are reduced but not yet negligible at these densities but they were overestimated in<sup>5</sup> as Fig. 3 shows. We consider the development of an improved analytical EOS model that better matches the DFT-MD simulation results a worthwhile future project but it goes beyond the scope of this article.

We did not extend our entropy calculations in Fig. 1 at 1000–3000 K to higher densities because simulations exhibited signs of spontaneous phase separation. The immiscibility of hydrogen and helium leads to helium rain in Saturn and Jupiter<sup>22</sup>. This process was studied with accurate TDI calculations that included the non-ideal entropy of mixing by Morales *et al.*<sup>11</sup>.

The snapshot from our simulations in Fig. 2 shows that this process can be observed directly in simulations of 220 H-18 He mixtures when they are performed for conditions that are sufficiently deep in the region of immiscibility. The system then spontaneously separates into a helium-rich and hydrogen-rich phase. We found that the best signature to identify this process is to look for a rise in the helium-helium pair correlation function at  $r = 1.5 \text{ \AA}$  and for a drop below 1 at large  $r$  as shown in Fig. 2. If the density is increased from  $r_s = 1.6$  to  $1.4$  at 3000 K, the peak in the hydrogen pair correlation function disappears and then the system assumes a metallic state<sup>23</sup>. The helium atoms then show a strong enough preference to form their own phase so that this process can be observed in simulations with only 18 helium atoms. We

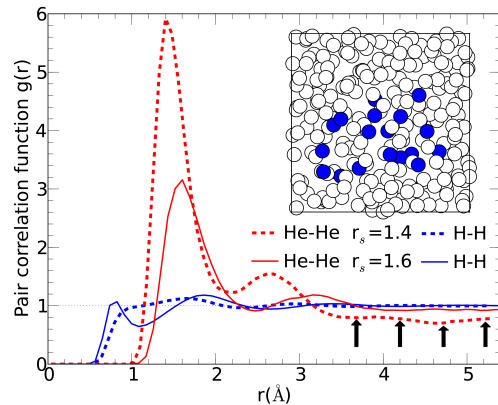


FIG. 2: Pair correlation functions at 3000 K for  $r_s=1.4$  and  $1.6$ . The inset shows H and He atoms respectively as light and dark spheres in a snapshot from a MD simulation at  $r_s=1.4$  where the system exhibits spontaneous H-He phase separation. This is supported by the drop in the He-He correlation function at large  $r$  (black arrows).

observed this process in the simulations with the Baldereschi point and with a  $2 \times 2 \times 2$  k-point grid. Upon decompression the system transforms back to a more mixed state. Our observations confirm the findings of Lorenzen *et al.*<sup>24</sup> who reported the spontaneous phase separation of HHM in MD simulations with much higher helium fraction at a higher density. Both sets of simulation results confirm the predictions in Ref. [11] but the exact  $(P, T)$  conditions are still better determined with the TDI method.

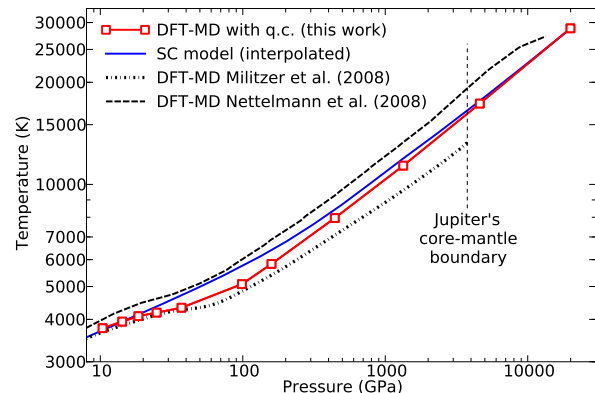


FIG. 3: Adiat for Jupiter's interior temperature-pressure profile.

In Fig. 3, we compare Jupiter's current adiabat for  $S = 7.0782 k_b/\text{el.}$ <sup>25</sup> derived from our DFT-MD simulations with the interpolated version of the SC model. We find excellent agreement in the high-pressure limit and very reasonable agreement at the lowest pressures. A small deviation remains around 10 GPa that is reminiscent of the entropy deviations in the molecular phase that we described in Fig. 1. The largest deviations occur near the molecular-to-metallic transition around 100 GPa where the SC model predicts temperatures for the adiabat that are 13% higher at fixed pressure than we derived from our DFT-MD simulations. This deviation is

in fact rather small and relies on the partial cancellation of errors. If one instead compares for fixed density and entropy, the SC model predicts temperatures and pressures that are 21% and 35% higher than our DFT-MD results, respectively.

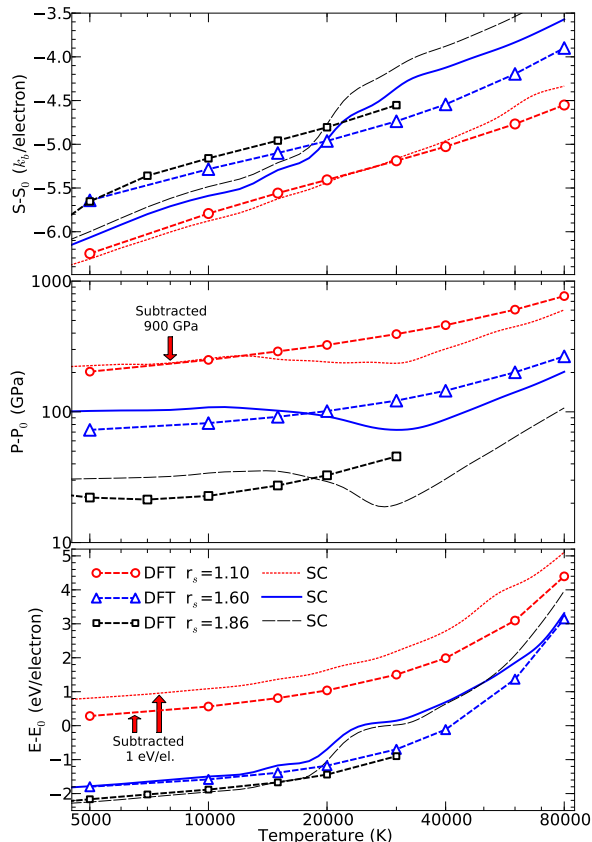


FIG. 4: Entropy, pressure, and internal energy of HHM. The contributions from an ideal gas of atoms were subtracted. For  $r_s=1.1$ , 1 eV was subtracted from the energy and 900 GPa from the pressure.

In Fig. 4, we compare the computed equation of state at high temperature conditions that correspond to the interiors of giant exoplanets and to the early stages of solar giant planets. The contributions from a non-interacting gas of spin-less hydrogen and helium atoms have been subtracted to remove a significant part of the temperature dependence so that deviations between both data sets can be discussed in more detail. The internal energy, pressure, and entropy are compared for three densities of  $r_s=1.1$ , 1.6, and 1.86. The latter two values were chosen in the vicinity of the molecular-to-metallic transition<sup>23</sup> where we have identified the largest deviations in Fig. 3.  $r_s=1.1$  corresponds to the deep interior of giant planets where the HHM is dense and very degenerate electronically. However, interaction effects are still too strong for idealized EOS models to work well.

We find excellent agreement for the internal energy be-

tween DFT-MD simulations and the SC model for  $r_s=1.6$  and 1.86 up to approximately 20 000 K. No stable molecules exist under these conditions, and one can conclude that the excitations from the thermal motion of nuclei are well described in the SC model. Above 20 000 K, one finds a rapid rise of about 1 eV/el. in the SC that is not present in the DFT-MD data. This discrepancy has been identified and discussed earlier when the SC model has been compared with path integral Monte Carlo (PIMC) simulations of dense hydrogen<sup>26</sup>. PIMC and DFT-MD have been shown to yield very similar EOSs for a number of materials<sup>27–30</sup>. The reason for the deviation is that the SC model underestimates the temperature interval, in which the electrons become free and atoms are ionized. These processes are all included in the DFT-MD and simulations but both predict them to occur gradually. When the evolution of a giant planet is simulated with the SC model, the temperature would remain nearly constant as the adiabat passes through this temperature interval because it would take some time before the significant amount of released heat could be removed convectively.

The difficulties in describing electronic excitation in the SC model have implications for other thermodynamic variables. The non-ideal pressure drops unphysically. The total pressure in the SC is overestimated at lower temperature and underestimated at high temperature. Similarly, the entropy is underestimated by  $\sim 0.3 k_B/\text{el.}$  below 20 000 K for  $r_s = 1.6$ , then rises quickly to become overestimated by  $\sim 0.4 k_B/\text{el.}$

For  $r_s = 1.1$ , the agreement between DFT-MD and SC is generally quite good but there is an offset in the internal energy of  $\sim 0.8 \text{ eV/el.}$  We confirm that this deviation by performing calculations with the Abinit code<sup>31</sup>, for which we can construct pseudopotentials with small core radii.

## IV. CONCLUSION

We have extended existing TDI techniques to study molecular hydrogen and applied this method to simulations with electronic excitations. This allows us to directly determine the entropy of hydrogen-helium mixtures over a wide range of pressure-temperature conditions in the interiors of solar and extrasolar giant planets. For the lowest and highest pressures, we find good agreement with the analytical SC EOS model but significant deviations have been identified at intermediate pressures and in the regime of ionization.

## Acknowledgments

We acknowledge support from NASA and NSF, computational resources from NCCS as well as discussions with W. B. Hubbard and K. P. Driver.

<sup>1</sup> W. Borucki *et al.* *Astrophys. J.*, 736:19, 2011.

<sup>2</sup> M. D. Knudson and M. P. Desjarlais. *Phys. Rev. Lett.*, 103:225501,

- 2009.
- <sup>3</sup> B. Militzer and W. B. Hubbard. *AIP Conf. Proc.*, 955:1395, 2007.
- <sup>4</sup> B. Militzer, W. H. Hubbard, J. Vorberger, I. Tamblyn, and S. A. Bonev. *Astrophys. J. Lett.*, 688:L45, 2008.
- <sup>5</sup> N. Nettelmann, B. Holst, A. Kietzmann, M. French, R. Redmer, and D. Blaschke. *Astrophys. J.*, 683:1217, 2008.
- <sup>6</sup> D. Saumon, G. Chabrier, and H. M. Van Horn. *Astrophys. J. Suppl.*, 99:713, 1995.
- <sup>7</sup> B. Militzer and W. H. Hubbard. *Astrophys. and Space Sci.*, 322:129, 2009.
- <sup>8</sup> N. Nettelmann, A. Becker, B. Holst, and R. Redmer. *Astrophys. J.*, 750:52, 2012.
- <sup>9</sup> P. E. Blöchl. *Phys. Rev. B*, 50:17953, 1994.
- <sup>10</sup> D. Alfè, M. J. Gillan, and G. D. Price. *Nature*, 405:172, 2000.
- <sup>11</sup> M. A. Morales, E. Schwegler, D. Ceperley, C. Pierleoni S. Hamel, K. Caspersen, *Proc. Nat. Acad. Sci.*, 106:1324, 2009.
- <sup>12</sup> H. F. Wilson and B. Militzer. *Phys. Rev. Lett.*, 104:121101, 2010.
- <sup>13</sup> H. F. Wilson and B. Militzer. *Astrophys. J.*, 745:54, 2012.
- <sup>14</sup> H. F. Wilson and B. Militzer. *Phys. Rev. Lett.*, 108:111101, 2012.
- <sup>15</sup> S. Izvekov, M. Parrinello, C. J. Burnham, and G. A. Voth. *J. Chem. Phys.*, 120:10896, 2003.
- <sup>16</sup> G. A. de Wijs, G. Kresse, and M. J. Gillan. *Phys. Rev. B*, 57:8223, 1998.
- <sup>17</sup> N. D. Mermin. *Phys. Rev.*, 137:A1441, 1965.
- <sup>18</sup> T. R. Mattsson and M. P. Desjarlais. *Phys. Rev. Lett.*, 97:017801, 2006.
- <sup>19</sup> R. M. Wentzcovitch, J. L. Martins, and P. B. Allen. *Phys. Rev. B*, 45:11372, 1992.
- <sup>20</sup> G. Kresse and J. Furthmüller. *Phys. Rev. B*, 54:11169, 1996.
- <sup>21</sup> J. P. Perdew, K. Burke, and M. Ernzerhof. *Phys. Rev. Lett.*, 77:3865, 1996.
- <sup>22</sup> D.J. Stevenson and E.E. Salpeter. *Astrophys. J. Suppl. Ser.*, 35:221, 1977.
- <sup>23</sup> M. A. Morales, C. Pierleoni, E. Schwegler, and D. M. Ceperley. *Proc. Nat. Acad. Sci.*, 107:12799, 2010.
- <sup>24</sup> W. Lorenzen, B. Holst, and R. Redmer. *Phys. Rev. B*, 84:235109, 2011.
- <sup>25</sup> G. F Lindal *et al.* *J. Geophys. R.*, 86:8721, 1981.
- <sup>26</sup> B. Militzer and D. M. Ceperley. *Phys. Rev. E*, 63:066404, 2001.
- <sup>27</sup> B. Militzer, D. M. Ceperley, J. D. Kress, J. D. Johnson, L. A. Collins, and S. Mazevet. *Phys. Rev. Lett.*, 87:275502, 2001.
- <sup>28</sup> B. Militzer. *Phys. Rev. Lett.*, 97:175501, 2006.
- <sup>29</sup> B. Militzer. *Phys. Rev. B*, 79:155105, 2009.
- <sup>30</sup> K. P. Driver and B. Militzer. *Phys. Rev. Lett.*, 108:115502, 2012.
- <sup>31</sup> X. Gonze *et al.* *Comp. Phys. Comm.*, 180:2582, 2009.